DFT study on Thiotepa and Tepa interactions with their DNA receptor

ARTICLE *in* STRUCTURAL CHEMISTRY · FEBRUARY 2013

Impact Factor: 1.84 · DOI: 10.1007/s11224-012-0020-4

2 AUTHORS, INCLUDING:

Hedieh Torabifard
Wayne State University
5 PUBLICATIONS **14** CITATIONS

SEE PROFILE

Struct Chem (2013) 24:1–11
DOI 10.1007/s11224-012-0020-4

ORIGINAL RESEARCH

DFT study on Thiotepa and Tepa interactions with their DNA receptor

Hedieh Torabifard · Alireza Fattahi

Received: 14 November 2011 / Accepted: 13 April 2012 / Published online: 6 May 2012

Abstract Thiotepa (*N,N′,N″*-triethylenethiophosphoramide) and its major metabolite (Tepa) as trifunctional alkylating agents has recently been used in cancer therapy. In vivo and vitro studies show the possible pathways of alkylation of DNA by Thiotepa and Tepa. Two pathways are suggested, but the main pathway of mechanism remains unclear. In pathway 1, forming cross-links with DNA molecules can be carried out via two different mechanisms. In first mechanism, these agents undergo the ring opening reaction which is initiated by protonating aziridine, which then becomes the main target of nucleophilic attack by the N7-Guanine of DNA. The second probable mechanism is ring opening of aziridyl group by nucleophilic attack of N7-Guanine without initial protonation. Thiotepa and Tepa in pathway 2, act as a cell penetrating carrier for aziridine, which is released via hydrolysis. The released aziridine can form a cross-link with N7-Guanine. In this study, we calculated the activation free energy and kinetic rate constant for alkylating the Guanine via the first pathway to determine the most precise mechanism by applying density functional theory using B3LYP method. We carried out geometrical optimizations with the conductor-like polarizable continuum model to account for the solvent effect, and the results were compared with those in the gas phase. Hyperconjugation stabilization factors that affect on stability of generated transition state were investigated by natural bond order analysis. Furthermore, quantum theory of atoms in molecules analysis was performed to extract the bond critical points properties because the electron densities can be considered as a good description of the strength of different types of interactions.

Keywords Density functional theory (DFT) · Thiotepa and Tepa · Anticancer drugs · Kinetic study · Alkylating agents

Introduction

The family of antitumor drugs based on Thiotepa (*N,N′,N″*-triethylenethiophosphoramide), has been the subject of several recent investigations (Fig. 1). Thiotepa drugs of general formula $(C_2H_4N)_3PX$ are alkylating agents whose antitumor action occurs mostly through alkylating the N7 position of Guanine base in DNA [1]. Following Miller's theory, the nucleophilic centers on the DNA interact with electrophilic species [2]. Although the reaction at the different sites strongly depends on the nucleophilicity of the DNA centers, the steric factors have important role. The most nucleophilic sites are endocyclic nitrogens such as N3- and N7-Guanine, while exocyclic base oxygens are less nucleophilic [3]. Guanine N7, exposed in the major groove of normal helical DNA, is more accessible and hence more able to react with electrophiles than N3 position. Therefore, the alkylation of DNA takes place on N7-Guanine [2].

Thiotepa has been applied in cancer therapy for more than 60 years [4]. Thiotepa has recently been employed in high-dose combination regimens for breast cancer, ovarian cancer, and other solid tumors, because of its broad spectrum anti-tumor activity [5]. Tepa (*N,N′,N″*-triethylenephosphoramide) was the first reported metabolic of

Electronic supplementary material The online version of this article (doi:10.1007/s11224-012-0020-4) contains supplementary material, which is available to authorized users.

H. Torabifard · A. Fattahi (✉)
Department of Chemistry, Sharif University of Technology, P.O. Box 11365-9516, Tehran, Iran
e-mail: fattahi@sharif.edu

Thiotepa, and is formed in the liver after oxidative desulfuration by cytochrome P450 (Fig. 1). It was first reported by Mellet and Woods in 1960 [6].

In vivo and vitro studies demonstrated that alkylation of Guanine by Thiotepa and Tepa can follow two pathways, but the precise mechanism of action remains unclear [5, 7–9]. Thiotepa as polyfunctional alkylating agent can form crosslink with DNA molecules according to pathways described in Fig. 2. Pathway 1 has two different reaction mechanisms. In the first mechanism, one of the aziridinyl groups takes a proton then ring opening reaction is carried out via nucleophilic attack by the N7 Guanine of DNA. The second one is direct nucleophilic ring opening of aziridinyl group. In pathway 2, Thiotepa and Tepa release aziridine via hydrolysis, and then the released aziridine can react with DNA on N7 Guanine [10, 11]. The reaction is a prototype for chemical modifications of the DNA induced by the alkylating agents.

In this study, we calculated the activation free energy and kinetic rate constant of first pathway in biological condition of body (pH 7.4) and in acidic pH of cancer cells (pH 4–6)

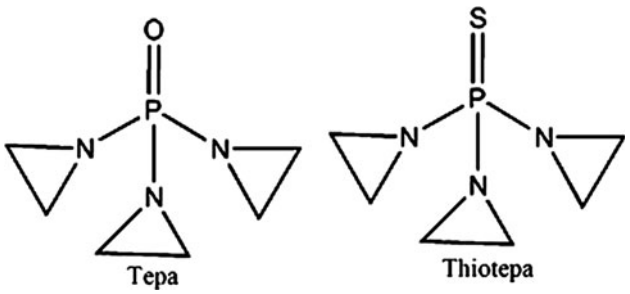

Fig. 1 The structure of Thiotepa and Tepa

[12]. Thiotepa and Tepa alkylates DNA mainly at N7 position of Guanine [13, 14] via the S_N2-substitution mechanism which is the rate-limiting step of the reaction. DNA was truncated to guanine, the chemically relevant part of entering the reaction. The protonation is believed to be a fast process due to a proton rich microenvironment surrounding DNA [15]. To our best knowledge, this is the first quantum-chemical calculation of the activation energy for a chemical reaction between a part of DNA and Thiotepa and Tepa.

In this study, activation free energies of the direct reaction between Thiotepa and Tepa with Guanine were calculated using density functional theory (DFT) and the rate constant k was obtained on the basis of the transition state theory [16]:

$$k = \frac{k_B T}{h} \times e^{-\frac{\Delta G^{\neq}}{k_B T}}$$

where k_B, h, and T represent Boltzmann constant, the Planck's constant, and the absolute temperature, respectively. Transition state theory is based on assumption that reactants and transition states form a thermal equilibrium. Its validity in biocatalysis was proven experimentally by the development of catalytic antibodies and theoretically by the success of empirical valence bond (EVB) method [17]. Because biochemical reactions do not take place in vacuum, solvation effects were incorporated in this study by the solvent reaction field method of Tomasi and co-workers [18].

Computational methods

Initial search of minima on the potential energy surface of reactants forms at the relative energy range of 10 kcal/mol

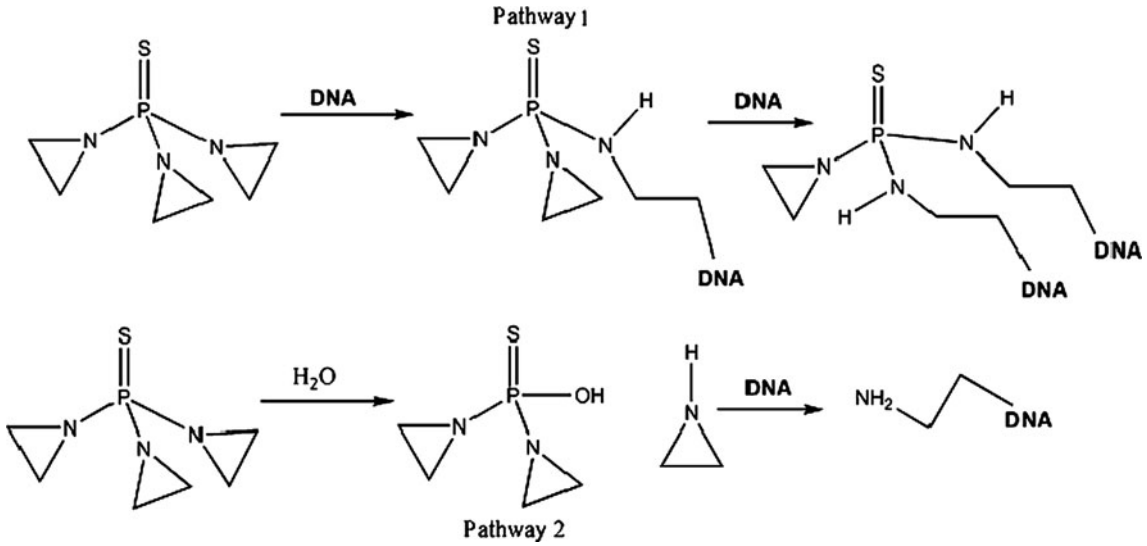

Fig. 2 Possible interaction of Thiotepa with DNA. *Pathway 1* formation of cross-links between Thiotepa and DNA. *Pathway 2* Thiotepa as a prodrug for aziridine

were carried out using the MMFF force field in the Spartan software [19]. The most stable conformers were optimized by the density functional (DFT) method using Becke3 (B3) exchange [20] and Lee, Yang, and Parr (LYP) correlation [21] potentials, in connection with the 6-311++G(d,p) orbital basis set as implemented in the Spartan software. This basis set was selected for all calculations as it contains both polarized basis set and diffuse functions. The analytical harmonic vibrational wave numbers for all structures were positive values, confirming that the local minima on the potential energy surface had been found. Transition states were explored employing the quadratic Berny algorithm. The transition state structures have a negative value for the analytical harmonic vibrational wave number.

Continuum solvation method was used for solvation free energies. The polarizable continuum model (PCM) [22] was applied using the conductor-like polarizable continuum variant (CPCM) [23]. CPCM calculations were performed with geometrical optimizations. Continuum models require a description of the shape and size of the cavity occupied by solute molecules in the solvent. Water, THF, and diethylether were modeled with a dielectric constant $\varepsilon = 80$, 8, and 4, to simulate the condition of cells [24–27]. Here, we have applied DFT calculations in combination with a cluster-continuum model to account for solvent effects, which has been shown to yield satisfactory solvation energies [28–30].

Natural bond order (NBO) analysis was carried out using the B3LYP functional and the 6-311++G (d,p) basis set. In this context, a study of hyperconjugative interactions has been completed. Hyperconjugation may be given as a stabilizing effect that arises from an overlap between an occupied orbital with another neighboring electron deficient orbital when these orbitals are properly oriented. This non-covalent bonding–antibonding interaction can be quantitatively described in terms of the NBO approach that is expressed by means of the second-order perturbation interaction energy ($E^{(2)}$) [31–35]. This energy represents the estimate of the off-diagonal NBO Fock matrix elements. It can be deduced from the second-order perturbation approach [35]:

$$E^{(2)} = \Delta E_{ij} = q_i \frac{F(i,j)^2}{\varepsilon_i - \varepsilon_j}$$

where, q_i is the donor orbital occupancy, ε_i; ε_j are diagonal elements (orbital energies) and $F(i,j)$ is the off-diagonal NBO Fock matrix element.

Furthermore, electron densities $\rho(r)$ and Laplacians $\nabla^2 \rho(r)$ of various interactions at bond critical points have been calculated at the 6-311++G (d,p) level using Bader's theory of atoms in molecules (AIM) [35, 36]. AIM is a very useful tool in analyzing hydrogen bonds and interactions, with a large electronic density at the critical point. In this paper, we calculated the electron density topological properties of our systems using the AIM2000 program [37]. According to the AIM theory, the presence of a hydrogen bond like any chemical bond must correspond to the existence of a bond path between the donor and the acceptor atoms containing the bond critical point (BCP), in topological analysis of the electron density distribution. Laplacian of $\rho(r)$ is related to the bond interaction energy by a local expression of the viral theorem [38]:

$$\left[\frac{\hbar^2}{4m}\right]\nabla^2\rho(r) = 2G(r) + V(r)$$

where $G(r)$ is the electronic kinetic energy density and $V(r)$ is the electronic potential energy density. A negative $\nabla^2 \rho(r)$ shows the excess potential energy at bond critical point (BCP). It means that electronic charge is concentrated in the inter-nuclear region, and therefore, shared by two nuclei. This is the case in all shared electron (covalent) interactions. A positive $\nabla^2 \rho(r)$, at a BCP reveals that the kinetic energy contribution is greater than that of potential energy, and shows depletion of electronic charge along the bond path. This is the case in all closed-shell electrostatic interactions [39, 40]. Furthermore, the electronic energy density $H(r)$ at BCP is defined as $H(r) = G(r) + V(r)$. The sign of $H(r)$ determines whether the accumulation of charge at a given point of r is stabilizing ($H(r) < 0$) or destabilizing ($H(r) > 0$). The bond energies E_X calculated by using the following equation:

$$E_X = 1/2V_{(r)} \quad V_{(r)} = 1/4\nabla^2\rho(r) - 2G(r)$$

Finally, the criterion nature of bonds evaluated by means of $-G(r)/V(r)$ ratio. When $-G(r)/V(r) > 1$ the interaction is noncovalent, while for $0.5 < -G(r)/V(r) < 1$ it is partly covalent [41, 42]. Moreover, Rozas et al. [43] have developed a new classification of the interactions. Weak interactions exhibit positive values for both $\nabla^2\rho(r)$ and $H(r)$, for medium interactions $\nabla^2\rho(r) > 0$ and $H(r) < 0$, and for strong interactions both $\nabla^2\rho(r)$ and $H(r)$ are negative. We use these criteria to characterize different interactions considered in this study. It's important to note that the AIM analysis is more practicable for hydrogen bonds but in the case of other interaction it can be useful.

Result and discussion

Gas phase

The mechanism of attack via initial protonation (in acidic pH)

The values of proton affinity for Thiotepa and Tepa (which are 225.0 and 225.8, respectively) confirm that these agents

can be protonated in acidic pH of cancer cells (i.e., pH 4–6) [12]. The protonation of one of the aziridinyl ring is considered as a very fast step and the rate-limiting step is the nucleophilic attack of Guanine on aziridinuim ring to form a cationic intermediate. The overall mechanism of attacking Guanine to Thiotepa via initial protonation is presented in Fig. 3.

The activation free energy is defined as a Gibbs free energy difference between the transition state and the reactants. To obtain the Gibbs free energy of activation of this step, we therefore need only to consider its reactants (Thiotepa or Tepa + Guanine in Fig. 3) and its transition states. The saddle point is characterized by a single imaginary frequency on the potential energy surface connecting reactants and the cationic intermediate.

In the first transition state (TS1, $\Delta G^{\#}_{(g)\text{Thiotepa}} = 11.6$ kcal/mol, $\Delta G^{\#}_{(g)\ \text{Tepa}} = 14.1$ kcal/mol, see Fig. 4) of this mechanism, the nucleophile Guanine attacks these agents (Thiotepa and Tepa), and cause the ring opening of one of the aziridinyl group. The intermediate (INT, $\Delta_r G_{(g)\text{Thiotepa}} = -27.7$ kcal/mol, $\Delta_r G_{(g)\text{Tepa}} = -30.7$ kcal/mol, Fig. 4, we consider related intermediate and reactant for $\Delta_r G$) is a cationic compound which can undergo two different mechanisms and yields species P1and P2 as products (Fig. 3). The Gibbs free energies (ΔG) for these two different mechanisms are presented in Table 1. As shown in Table 1, the mechanism 1 is thermodynamically more favorable than mechanism 2. It is important to mention that the intramolecular cyclization is not recognized experimentally. However, the intermediate was observed as main alkylated products [7]. Therefore, it seems that reaction stops at formation of intermediate. Consequently, further calculation was abandoned.

The mechanism of attack without initial protonation (in physiological pH)

Our calculations focus on the first step of the reaction between Thiotepa and Tepa with Guanine in pH of normal cells (Fig. 5) as this S_N2-substitution represents the rate-limiting step. It leads to the formation of the relatively unstable zwitterionic intermediate.

The data (TS1, $\Delta G^{\#}_{(g)\ \text{Thiotepa}} = 26.9$ kcal/mol, $\Delta G^{\#}_{(g)\ \text{Tepa}} = 44.3$ kcal/mol, Fig. 6) demonstrate this fact that the energy barriers in acidic pH are less than these values in physiological pH. Therefore, the alkylation mechanism of Guanine takes place faster in cancer cells (pH 4–6).

The comparison between the $\Delta G^{\#}_{(g)}$ values and kinetic rate constants is presented in Table 2. The huge differences between the rate constants in acidic and normal pH are rationalized by the strain on the aziridinuim ring in low pH. In fact, Thiotepa and Tepa in acidic condition react with Guanine rapidly to lower the strain on aziridinuim ring.

As discussed in previous section, there might be two different mechanisms for the zwitterionic intermediate to yield two different products as presented in Fig. 5. As shown in acidic condition, the instability of product in the intramolecular cyclization confirms that this mechanism is not a probable mechanism. On the other hand, the reaction may stop after first step and intermediate remains ionic. Therefore, more calculation in this regard was abandoned.

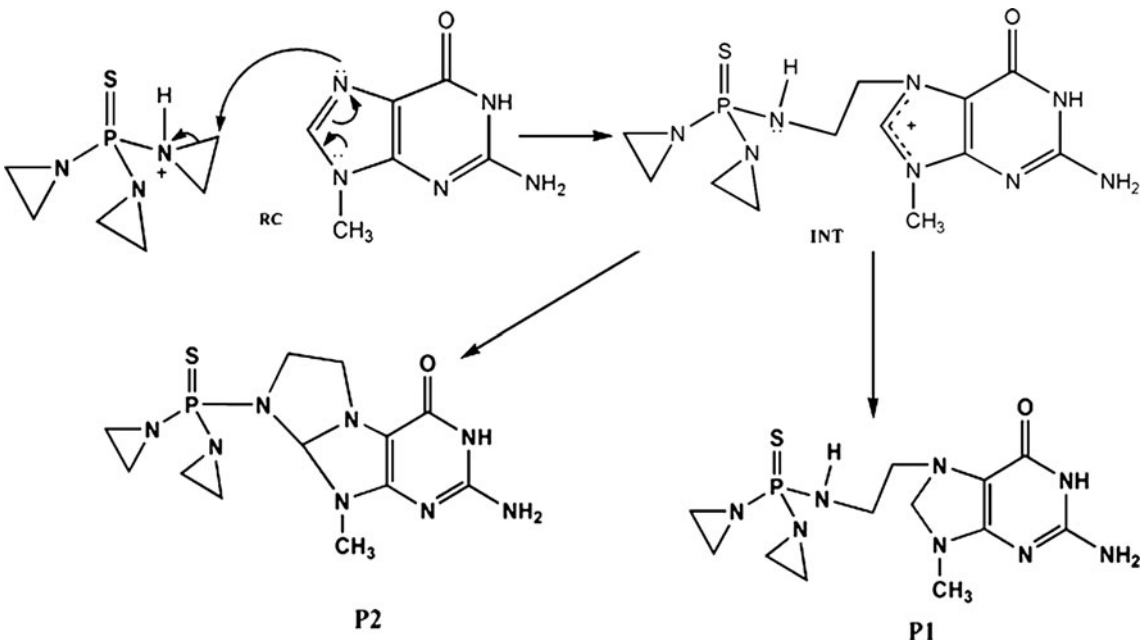

Fig. 3 The mechanism of attack via initial protonation (in acidic pH)

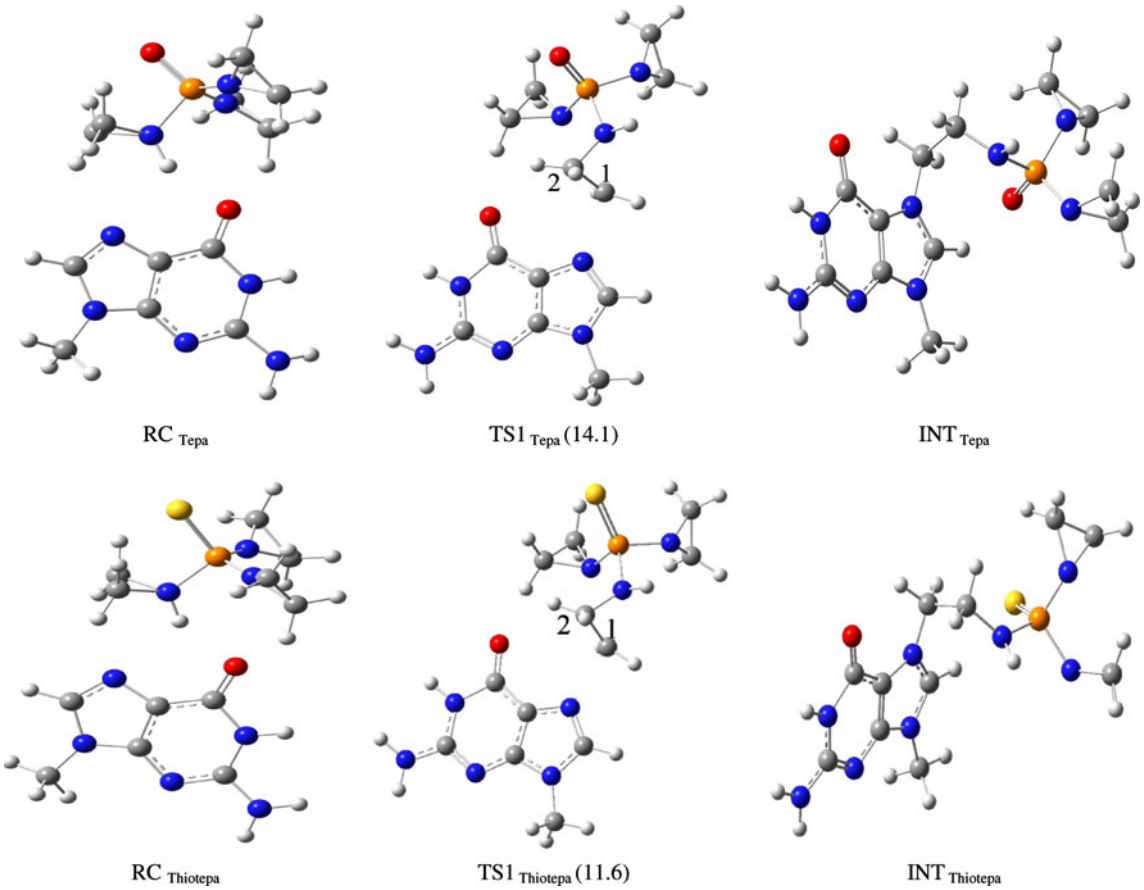

Fig. 4 Optimized geometries of stationary points for Tepa and Thiotepa in gas phase in acidic pH. Values in *parentheses* are Gibbs free energies of activation ($\Delta G^{\#}$) in gas-phase at 298 k (kcal/mol)

Table 1 B3LYP/6-311++G (d,p) Gibbs free energies (ΔG, in a.u. and kcal/mol), of two different suggested mechanisms of attack via initial protonation (in acidic pH)

Mechanism	ΔG (a.u.)	ΔG (kcal/mol)
1	−0.2301	−144.4
2	0.4075	255.7

NBO and AIM analysis

NBO analysis shows that there are some hyperconjugation interactions between bonding and antibonding orbitals in acidic condition which are in coincidence with the obtained kinetic results. For example, in transition state structure, the second-order energy of $n \rightarrow \sigma^*$ type of interactions is $n_{\mathrm{N7(Gua)}} \rightarrow \sigma^*_{\mathrm{C1\text{-}NH(Thiotepa)}}$ (45.2 kcal/mol, Fig. 4), which indicates that this reaction proceeds via S_N2 mechanism. The interactions between $n_{(2)\mathrm{O(Gua)}} \rightarrow \sigma^*_{\mathrm{NH(Thiotepa)}}$ and $n_{\mathrm{N7(Gua)}} \rightarrow \sigma^*_{\mathrm{NH(Thiotepa)}}$ in reactant are 6.8 and 1.4 kcal/mol, respectively. These interactions indicate the presence of hydrogen bonds in reactant of Thiotepa in acidic condition as shown in Fig. 4. In addition, AIM analysis has the same results. AIM analysis in acidic condition (see Table 3) shows that in reactant for Thiotepa there are weak hydrogen bonds ($\nabla^2\rho(r)$ and $H(r) > 0$) between hydrogen atom of aziridinuim ring of Thiotepa and oxygen and nitrogen atoms (N7) of Guanine (4.8 and 1.5 kcal/mol, respectively). These weak hydrogen bonds have positive effect in proceeding the mechanism, because Thiotepa is located in suitable situation of attack by Guanine. Therefore, the mechanism proceeds faster and $\Delta G^{\#}$ becomes lower in acidic condition. The medium interaction in transition state with $\nabla^2\rho(r) > 0$ and $H(r) < 0$ (9.9 kcal/mol) indicates the Guanine as nucleophile attacks to aziridinuim ring to open it and thus reduce its strain. There are similar results in the case of Tepa, especially in reactants because the type of hydrogen bonds on Thiotepa and Tepa are completely similar. The interaction between $n_{(2)\mathrm{O(Gua)}} \rightarrow \sigma^*_{\mathrm{NH(Tepa)}}$, $n_{(1)\mathrm{O(Gua)}} \rightarrow \sigma^*_{\mathrm{NH(Tepa)}}$, $n_{\mathrm{N7(Gua)}} \rightarrow \sigma^*_{\mathrm{NH(Tepa)}}$ in reactant and $n_{\mathrm{N7(Gua)}} \rightarrow \sigma^*_{\mathrm{C1\text{-}NH(Tepa)}}$ in transition state are 7.2, 2.0, 1.1, and 44.3 kcal/mol, respectively (see Fig. 4). The results obtained from AIM analysis confirm these results, see Table 3 for more details.

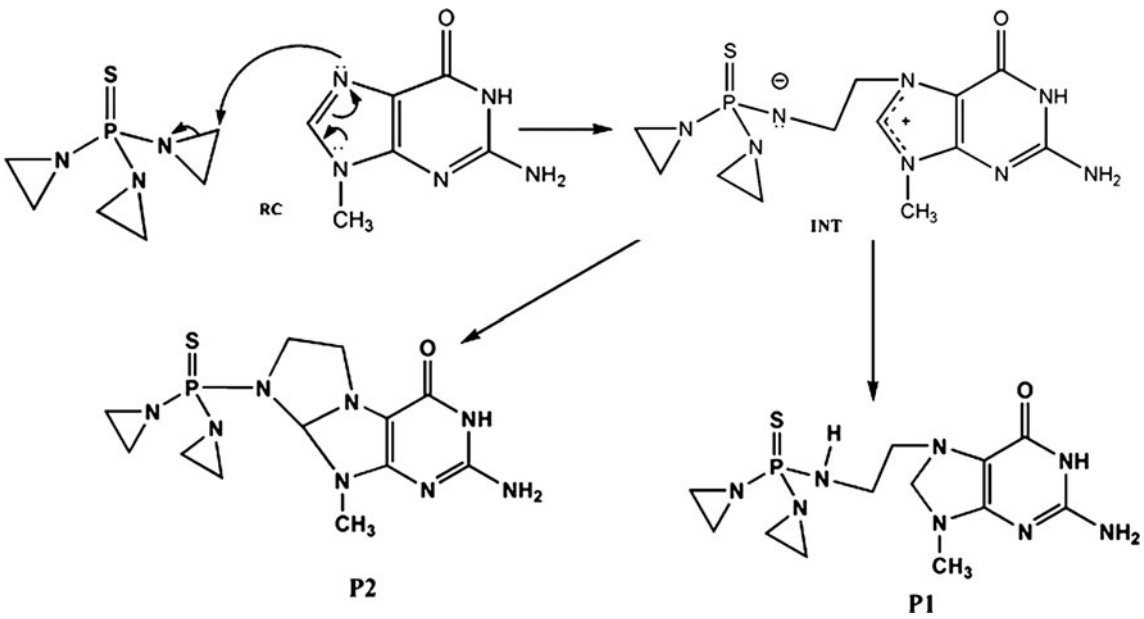

Fig. 5 The mechanism of attack without initial protonation (in physiological pH)

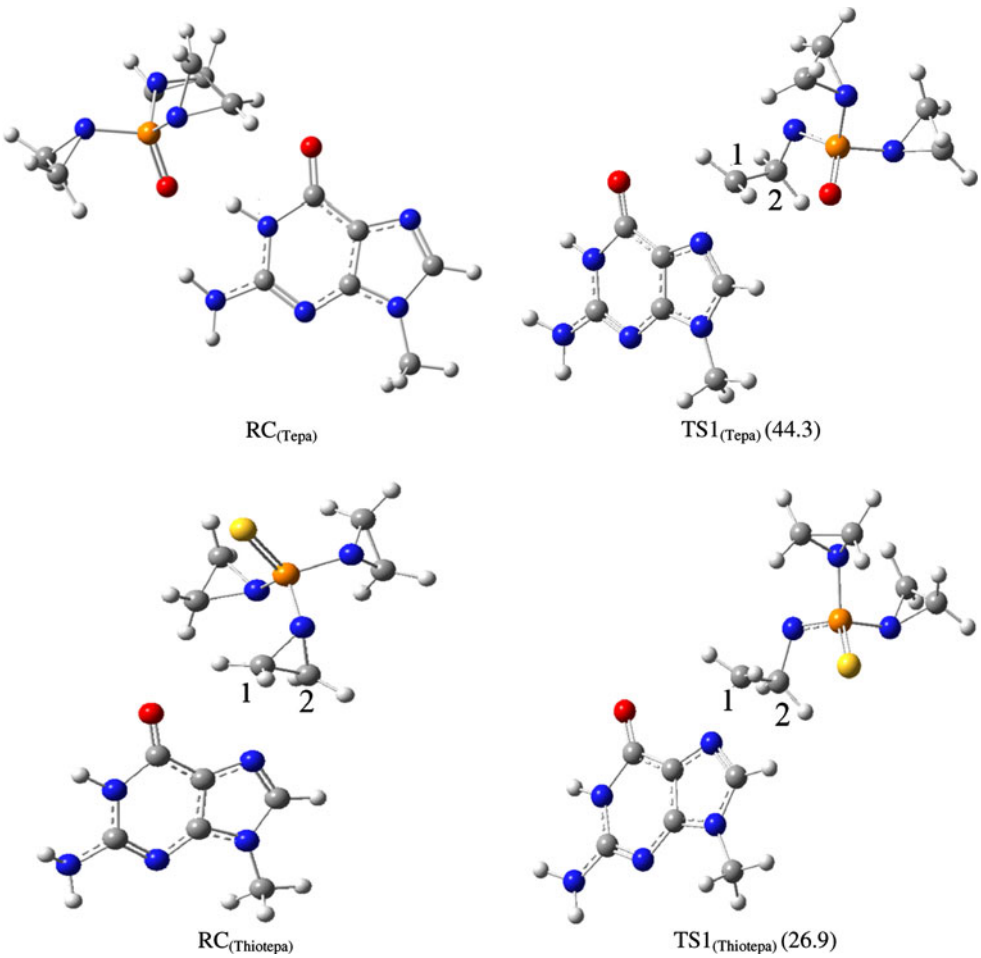

Fig. 6 Optimized geometries of stationary points for Tepa and Thiotepa in gas-phase in neutral pH. Values in *parentheses* are Gibbs free energies of activation ($\Delta G^{\#}$) in gas-phase at 298 k (kcal/mol)

The NBO analysis for Thiotepa in physiological pH shows the negligible values for the interactions, therefore we focus on the results of AIM analysis. As shown in Fig. 6, there are no hydrogen bonds in reactant and transition state for Thiotepa, but the weak interaction between C1 of Thiotepa and nitrogen atom (N7) of Guanine in reactants becomes more stronger in transition state, indicating the reaction proceed via S_N2 mechanism (see Table 3). In addition, reactant of Tepa in physiological pH has the hydrogen bonds between oxygen atom of Tepa and N1 and $N_{(exo)}$ of Guanine, which is confirmed by the AIM analysis. AIM analysis shows that both hydrogen bonds in the reactants are weak but it is important to note that $N1–H_{(Gua)}\cdots O_{(Tepa)}$ hydrogen bond (9.5 kcal/mol, Fig. 6) are stronger than $N_{(exo)}–H_{(Gua)}\cdots O_{(Tepa)}$ hydrogen bond (2.3 kcal/mol, Fig. 6). As shown in Fig. 6, these two hydrogen bonds are located in unpredicted situation and the large value of barrier for Tepa in neutral condition is

Table 2 Gibbs free energies of activation and kinetic rate constants in gas phase at 298 k in acidic and neutral pH

	$\Delta G^{\#}_{(g)}$(kcal/mol)	$k_{(g)}$ (s^{-1})
Neutral condition		
Thiotepa	26.9	1.01×10^{-7}
Tepa	44.3	1.60×10^{-20}
Acidic condition		
Thiotepa	11.6	1.82×10^{4}
Tepa	14.1	2.63×10^{2}

Table 3 The electron densities ($\rho(r)$, e/au^3), their Laplacians ($\nabla^2\rho(r)$, e/au^5), kinetic energy densities $G(r)$, potential energy densities $V(r)$, and electronic energy densities $H(r)$, hydrogen bond energies ($E_{(X)}$, kcal/mol) and $-G(r)/V(r)$ ratio at the BCPs in reactant and transition state

	Molecule	BCP	$\rho(r)$	$\nabla^2\rho(r)$	$G(r)$	$H(r)$	$V(r)$	$E_{(X)}$	$-G(r)/V(r)$
Acidic condition	RC(Tepa)	$N7_{(Gua)}\cdots H_{(az)}$	0.0086	0.0286	0.0060	0.0011	−0.0049	1.5	1.2
		$O_{(Gua)}\cdots H_{(az)}$	0.0228	0.0743	0.0170	0.0015	−0.0155	4.9	1.1
	TS (Tepa)	$N7_{(Gua)}–C1_{(Tepa)}$	0.0447	0.1040	−0.0260	−0.0027	−0.0315	9.9	0.9
	RC(Thiotepa)	$N7_{(Gua)}\cdots H_{(az)}$	0.0086	0.0277	0.0058	0.0011	−0.0047	1.5	1.2
		$O_{(Gua)}\cdots H_{(az)}$	0.0225	0.0731	0.0167	0.0015	−0.0152	4.8	1.1
	TS (Thiotepa)	$N7_{(Gua)}–C1_{(Thiotepa)}$	0.0449	0.1040	0.0288	−0.0028	−0.0317	9.9	0.9
Neutral condition	RC(Tepa)	$N1–H_{(Gua)}\cdots O_{(Tepa)}$	0.0350	0.1226	0.0305	0.0001	−0.0304	9.5	1.0
		$N_{(exo)}–H_{(Gua)}\cdots O_{(Tepa)}$	0.0116	0.0439	0.0092	0.0018	−0.0074	2.3	1.2
	TS (Tepa)	$N7_{(Gua)}–C1_{(Tepa)}$	0.0838	0.1012	0.0492	−0.0239	−0.0731	22.9	0.7
	RC(Thiotepa)	$N7_{(Gua)}–C1_{(Thiotepa)}$	0.0045	0.0130	0.0027	0.0005	−0.0022	0.7	1.2
	TS (Thiotepa)	$N7_{(Gua)}–C1_{(Thiotepa)}$	0.0810	0.1041	0.0479	−0.0218	−0.0697	21.9	0.7

Gua guanine, *az* aziridinuim ring of Thiotepa and Tepa

Table 4 Gibbs free energies and kinetic rate constants in three different solvents with dielectric constant $\varepsilon = 80$, 8, and 4

	$\Delta G^{\#}_{(aq)}$	$\Delta G^{\#}_{(THF)}$	$\Delta G^{\#}_{(DE)}$	$\Delta G^{\#}_{(g)}$
Neutral condition				
Thiotepa	20.4	25.2	25.9	26.9
Tepa	35.7	20.2	20.6	44.3
Acidic condition				
Thiotepa	9.5	9.6	9.7	11.6
Tepa	9.0	8.3	8.5	14.1
	$k_{(aq)}$ (s^{-1})	$k_{(THF)}$ (s^{-1})	$k_{(DE)}$ (s^{-1})	$k_{(g)}$(s^{-1})
Neutral condition				
Thiotepa	6.11×10^{-3}	1.80×10^{-6}	5.48×10^{-7}	1.01×10^{-7}
Tepa	3.39×10^{-14}	8.57×10^{-3}	4.35×10^{-3}	1.60×10^{-20}
Acidic condition				
Thiotepa	6.38×10^{5}	5.38×10^{5}	4.54×10^{5}	1.82×10^{4}
Tepa	1.49×10^{6}	4.87×10^{6}	3.47×10^{6}	2.63×10^{2}

$\Delta G^{\#}$ in kcal/mol, k in s^{-1}

rationalized by stability of reactant and difficulty of nucleophilic attack. In addition, the results of NBO analysis confirm the hydrogen bonds. For example, $n_{(1)O(Tepa)} \rightarrow \sigma^*_{N(exo)\text{-}H(Gua)}$ (7.7 kcal/mol, Fig. 6), $n_{(2)O(Tepa)} \rightarrow \sigma^*_{N1\text{-}H(Gua)}$ (10.8 kcal/mol, Fig. 6) and $n_{(1)O(Tepa)} \rightarrow \sigma^*_{N(exo)\text{–}H(Gua)}$ (1.2 kcal/mol, Fig. 6) in reactant and $n_{N7(Gua)} \rightarrow \sigma^*_{N\text{-}C1(Tepa)}$ (136.0 kcal/mol, Fig. 6) in transition state show the critical interactions.

Solution phase

The biological activity of a drug is usually tested in the aqueous rather than the gas phase, and the protonated form of the molecule may also differ from the form it adopts in the isolated state [44]. Therefore, the activation free energies for all suggested mechanisms were calculated in three different solvents using CPCM model.

The mechanism of attack via initial protonation (in acidic pH)

To approximately estimate the energetic effects that are not included in the quantum-chemical model, we applied a homogeneous dielectric field according to the CPCM method [45–48] with three dielectric constants, 4, 8, 80. As seen in Table 4, the barrier of the first step for thio analog is slightly reduced to 9.7 and 9.6 and 9.5 kcal/mol, for $\varepsilon = 4$, 8, and 80, respectively. Although the similar pattern is observed for Tepa (Table 4), the reduction of barriers in condensed media (water, THF, diethyl ether) for Tepa is more than Thiotepa. The optimized structures of transition states and reactant for Thiotepa and Tepa in water are presented in Fig. 7 and the optimized structures in two other solvents are presented in the supporting information. The mentioned hydrogen bondings in reactants of Thiotepa

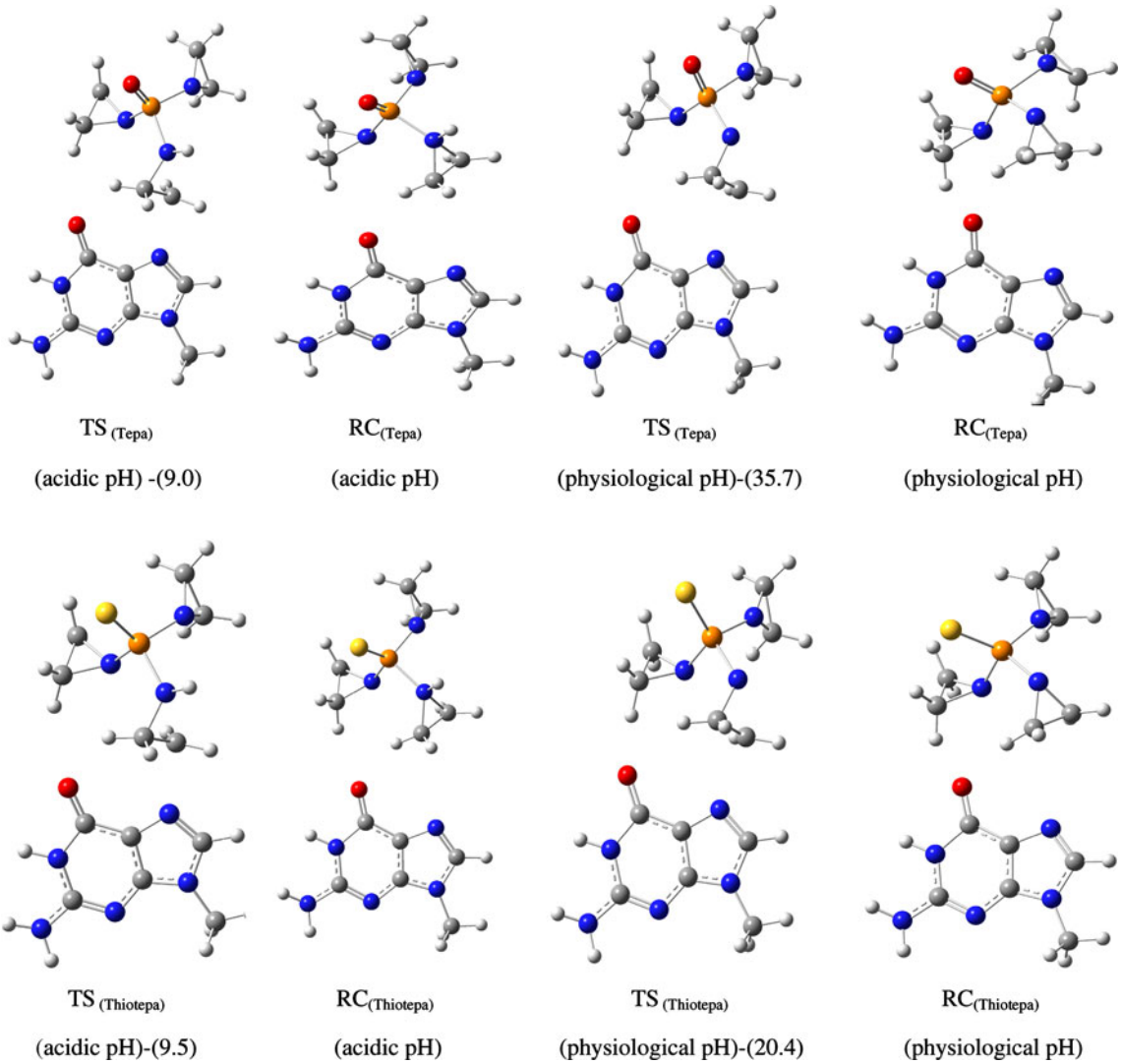

Fig. 7 Optimized geometries of stationary points for Tepa and Thiotepa in aqueous phase in neutral and acidic pH. Values in *parentheses* are Gibbs free energies of activation ($\Delta G^{\#}$) in aqueous-phase at 298 k (kcal/mol)

Table 5 Aqueous affect on the transition state and reactant of Thiotepa and Tepa in acidic and neutral condition

	Structure	μ (aqueous)	μ (gas)
Neutral condition	Thiotepa (TS)	20.2	13.8
	Thiotepa (RC)	14.6	12.4
	Tepa (TS)	19.3	14.6
	Tepa (RC)	16.5	12.1
Acidic condition	Thiotepa (TS)	9.8	7.8
	Thiotepa (RC)	3.7	3.9
	Tepa (TS)	10.3	8.2
	Tepa (RC)	3.3	2.7

and Tepa in gas phase (see Fig. 4) are disappeared in solution phase. This is the main difference between optimized structures in gas phase and solution.

Water as solvent has two different effects on reactant and transition state: (i) this polar solvent causes more stability of reactants due to localized charge on aziridinuim ring, (ii) water also can form hydrogen bond with hydrogen atom connected to the nitrogen atom of aziridinuim ring. It's important to note that hydrogen bonding stability is more in transition state than that in reactant because of the longer and weaker P–N bond in transition state. The decrease of values of barriers for Thiotepa and Tepa in water shows that the hydrogen bonding causes more stability of transition state than the reactant due to polarity of solvent.

On the other hand, it is known that a larger value of the dipole moment indicates more stabilization when the complex is exposed to a polar solvent-like water. As seen in acidic section in Table 5, the values of dipole moment in transition state increase from gas phase to aqueous phase, while they approximately remain stable in reactants for both agents. Hence, we can predict that transition states will become much more stable, whereas reactant of Thiotepa will become quite unstable in solvent surroundings. Consequently, the barriers in water decrease.

In addition, THF and diethylether as nonpolar solvent effect more on transition state due to distributed positive charge of aziridinuim ring. Therefore, transition state structure becomes more stable in these nonpolar solvents and barriers reduce.

The mechanism of attack without initial protonation (in physiological pH)

In this condition, the S_N2 mechanism results in formation of the relatively unstable zwitterionic intermediate. The CPCM solvation effects are more significant on Thiotepa as the barrier is significantly reduced to 25.9, 25.2, and 20.4 kcal/mol, for $\varepsilon = 4$, 8, and 80, respectively. The optimized structure of transition states and reactant for Thiotepa and Tepa in water are presented in Fig. 7. The

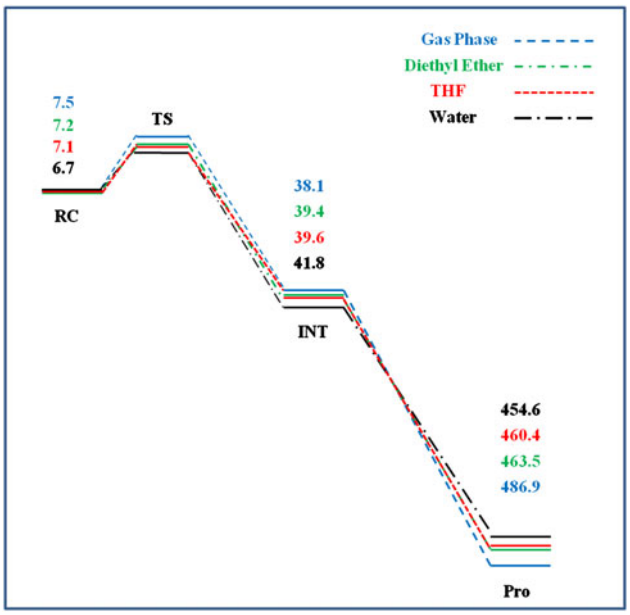

Fig. 8 The schematic potential energy surface of Thiotepa in gas-phase and solution (the values are free energies of activation (E_a) in kcal/mol)

optimized structures of two other solvents are presented in the supporting information.

In the case of Tepa, the barriers in solution phase are reduced dramatically to 20.6, 20.2, 35.7 kcal/mol, for $\varepsilon = 4$, 8, and 80, respectively. These changes in solution phase are rationalized by disappearance of hydrogen bondings between oxygen atom of Tepa and nitrogen atoms of Guanine which are observed in gas phase. In other words, the difficulty of nucleophilic attack by Guanine is omitted (Compare Figs. 6, 7).

Interestingly, the barriers in aqueous solution behave differently. Although the barriers in aqueous solution reduce for both agents in both conditions, their reduction in neutral condition is more than that in acidic condition. This observation can be rationalized by the different changes of dipole moments of transition states and reactant in physiological and acidic pH (Table 5). As seen in Table 5, the changes of dipole moment values in transition state for

both agents are more in neutral condition than those in acidic condition. Therefore, water as solvent decreases the barriers in neutral condition more.

Finally, the comparison between Gibbs free energies and kinetic rate constants of both agents in acidic and neutral condition are presented in Table 4. In addition, the schematic potential energy surface for comparison of gas- and solution-phase for Thiotepa in acidic condition are presented in Fig. 8 to perceive the effects of solvents better.

Conclusion

This study leads us to the following conclusions:

1. Alkylation reactions of Thiotepa and Tepa on Guanine could proceed via S_N2 type's mechanisms. These agents react faster in acidic pH which is rationalized by the high strain on aziridinuim ring.
2. The barrier energies for the alkylation reactions decrease substantially in going from gas phase to solution phase in both acidic and neutral conditions.
3. Tepa in physiological pH in gas phase showed the highest free energy (44.3 kcal/mol), indicating that it does not significantly contribute to the total rate of reaction. Therefore, the acidic condition is kinetically more favorable for Tepa than the neutral condition which the activation free energy is $\sim$30 kcal/mol lower than its value in neutral condition.

The predictive strategy presented here can in general be applied to prediction of suitable mechanism of anticancer drugs.

Acknowledgment Support from Sharif University of Technology is gratefully acknowledged. We thank Z. Aliakbar Tehrani, M. Jebeli Javan and M. Shakourian-Fard, Ph.D. students of Physical Organic Chemistry Laboratory at Sharif University of Technology.

References

1. Katzung BG (1998) Basic and clinical pharmacology, 7th edn. Prentice Hall, Englewood Cliffs, NJ
2. Benigni R, Bossa C (2010) Mechanisms of chemical carcinogenicity and mutagenicity: a review with implications for predictive toxicology. Chem Rev 111:2507–2536
3. Pullman B (1980) Carcinogenesis: fundamental mechanisms and environmental effects. D Reidel, Dordrecht, pp 51–55
4. Sykes M, Karnofsky D, Phillips F, Burchenal JH (1953) Clinical studies of triethylene-phosphoramide and diethylene-phosphoramide compounds with nitrogen mustard-like activity. Cancer 6:142–148
5. Van der Wall E, Beijnen JH, Rodenhuis S (1995) High-dose chemotherapy regimens for solid tumors. Cancer Treat Rev 21:105–132
6. Mellet LB, Woods LA (1960) The comparative physiological disposition of thiotepa and tepa in the dog. Cancer Res 20:524–532
7. Van Maanen MJ, Smeets CJM, Beijnen JH (2000) Chemistry, pharmacology and pharmacokinetics of *N,N',N"*-triethylenethiophosphoramide (ThioTEPA). Cancer Treat Rev 26:257–268
8. Van Maanen MJ, Tijhof IM, Damen JMA et al (1999) A search for new metabolites of *N,N',N"*-triethylenethiophosphoramide. Cancer Res 59:4720–4724
9. Van Maanen MJ, Doesburg Smits K, Damen JMA et al (2000) Stability of Thiotepa and its metabolites, TEPA, monochloro-TEPA and thioTEPA-mercapturate, in plasma and urine. Int J Pharm 200:187–194
10. Musser SM, Pan SS, Egorin MJ et al (1992) Alkylation of DNA with aziridine produced during the hydrolysis of *N,N',N''*-triethylenethiophosphoramide. Chem Res Toxicol 5:95–99
11. Hemminki K (1984) Reactions of ethyleneimine with guanosine and deoxyguanosine. Chem Biol Interact 48:249–260
12. Hunt CA, MacGregor RD, Siegal RA (1986) Engineering targeted in vivo drug delivery I. The physiological & physicochemical principles governing opportunities & limitations. Pharm Res 3:333–344
13. Segerback D, Calleman CJ, Schroeder JL, Costa LG, Faustman EM (1995) Formation of N-7-(2-carbamoyl-2-hydroxyethyl) guanine in DNA of the mouse and the rat following intraperitoneal administration of [14C] acrylamide. Carcinogenesis 16:1161–1165
14. Gamboa da Costa G, Churchwell MI, Hamilton LP, Von Tungeln LS, Beland FA, Marques MM (2003) DNA adduct formation from acrylamide via conversion to glycidamide in adult and neonatal mice. Chem Res Toxicol 16:1328–1337
15. Johnson WW, Guengerich FP (1997) Reaction of aflatoxin B1 exo-8,9-epoxide with DNA: kinetic analysis of covalent binding and DNA-induced hydrolysis. Proc Natl Acad Sci USA 94:6121–6125
16. Twaddle NC, McDaniel LP, Gamboa da Costa G, Churchwell MI, Beland FA, Doerge DR (2004) Determination of acrylamide and glycidamide serum toxicokinetics in B6C3F1 mice using LC-ES/MS/MS. Cancer Lett 207:9–17
17. Warshel A (1991) Computer modeling of chemical reactions in enzymes and solutions. Wiley, New York
18. Miertus S, Scrocco E, Tomasi J (1981) Electrostatic interaction of a solute with a continuum. A direct utilization of ab initio molecular potentials for the prevision of solvent effects. Chem Phys 55:117–129
19. Spartan'06V102' Wavefunction Inc., Irvine
20. Becke AD (1993) Density-functional thermochemistry. III. The role of exact exchange. J Chem Phys 98:5648–5652
21. Lee C, Yang W, Parr RG (1988) Development of the Colle-Salvetti correlation-energy formula into a functional of the electron density. Phys Rev B 37:785–789
22. Cossi M, Barone V, Mennucci B, Tomasi J (1998) Ab initio study of ionic solutions by a polarizable continuum dielectric model. Chem Phys Lett 286:253–260
23. Cossi M, Rega N, Scalmani G, Barone V (2003) Energies, structures, and electronic properties of molecules in solution with the C-PCM solvation model. J Comput Chem 24:669–681
24. Sevastik R, Himo F (2007) Quantum chemical modeling of enzymatic reactions: the case of 4-oxalocrotonate tautomerase. J Bioorg Chem 35:444–457
25. Georgieva P, Himo F (2008) Density functional theory study of the reaction mechanism of the DNA repairing enzyme alkylguanine alkyltransferase. Chem Phys Lett 463:214–218
26. Chen S, Fang w, Himo F (2008) Technical aspects of quantum chemical modeling of enzymatic reactions: the case of phosphotriesterase. Theor Chem Account 120:515–522

27. Himo F, Guo J, Rinaldo-Matthis A, Nordlund P (2005) Reaction mechanism of deoxyribonucleotidase: a theoretical study. J Phys Chem B 109:20004–20008
28. Pliego JR (2004) Basic hydrolysis of formamide in aqueous solution: a reliable theoretical calculation of the activation free energy using the cluster-continuum model. Chem Phys 306(1–3): 273–280
29. Stare J, Henson NJ, Eckert J (2009) Mechanistic aspects of propene epoxidation by hydrogen peroxide. Catalytic role of water molecules, external electric field, and zeolite framework of TS-1. J Chem Inf Model 49(4):833–846
30. Nguyen MT, Raspoet G, Vanquickenborne LG (1999) Necessity to consider a three-water chain in modelling the hydration of ketene imines and carbodiimides. J Chem Soc 4:813–820
31. Reed AE, Weinhold F (1985) Natural localized molecular orbitals. J Chem Phys 83:1736–1740
32. Reed AE, Weinstock RB, Weinhold F (1985) Natural population analysis. J Chem Phys 83:735–746
33. Reed AE, Weinhold F (1983) Natural bond orbital analysis of near-Hartree–Fock water dimer. J Chem Phys 78:4066–4073
34. Foster JP, Weinhold F (1980) Natural hybrid orbitals. J Am Chem Soc 102:7211–7218
35. Chocholousova J, Vladimir Spirko V, Hobza P (2004) First local minimum of the formic acid dimer exhibits simultaneously red-shifted O–H···O and improper blue-shifted C–H···O hydrogen bonds. Phys Chem Chem Phys 6:37–41
36. Reed AE, Curtiss LA, Weinhold F (1988) Intermolecular interactions from a natural bond orbital, donor–acceptor viewpoint. Chem Rev 88:899–926
37. Bader RFW (2002) AIM2000 program package, Ver. 2.0. McMaster University, Hamilton
38. Bader RFW (1998) Bond path: a universal indicator of bonded interactions. J Phys Chem A 102:7314–7323
39. Bader RFW (1990) Atoms in molecules. A quantum theory. Clarendon, Oxford
40. Pakiari AH, Eskandari K (2006) The chemical nature of very strong hydrogen bonds in some categories of compounds. J Mol Struct 759:51–60
41. Abboud JLM, Mó O, De Paz JLG et al (1993) Thiocarbonyl versus carbonyl compounds: a comparison of intrinsic reactivities. J Am Chem Soc 115:12468–12476
42. Hocquet A (2001) Intramolecular hydrogen bonding in 2′-deoxyribonucleosides: an AIM topological study of the electronic density. Phys Chem/Chem Phys 3:3192–3199
43. Rozas I, Alkorta I, Elguero J (2000) Behavior of ylides containing N, O, and C atoms as hydrogen bond acceptors. J Am Chem Soc 122:11154–11161
44. Kheffache D, Oumerali O (2010) Some physicochemical properties of the antitumor drug Thiotepa and its metabolite Tepa as obtained by density functional theory (DFT) calculations. J Mol Model 16:1383–1390
45. Barone V, Cossi M (1998) Quantum Calculation of Molecular Energies and Energy Gradients in Solution by a Conductor Solvent Model. Phys Chem A 102(11):1995–2001
46. Cammi R, Mennucci B, Tomasi J (1999) Second-Order Møller-Plesset Analytical Derivatives for the Polarizable Continuum Model Using the Relaxed Density Approach. Phys Chem A 103(45):9100–9108
47. Klamt A, Schüürmann G (1993) COSMO: a new approach to dielectric screening in solvents with explicit expressions for the screening energy and its gradient. Chem Soc, Perkin Trans 2:799–805
48. Tomasi J, Mennucci B, Cammi R (2005) Quantum Mechanical Continuum Solvation Model. Chem Rev 105(8):2999–3094